

Micro-patterned cell-sheets fabricated with stamping-force-controlled micro-contact printing



Nobuyuki Tanaka ^{a, b}, Hiroki Ota ^a, Kazuhiro Fukumori ^a, Jun Miyake ^b, Masayuki Yamato ^a, Teruo Okano ^{a, *}

^a Institute of Advanced Biomedical Engineering and Science, TWIns, Tokyo Women's Medical University, 8-1 Kawada-cho, Shinjuku-ku, Tokyo 162-8666, Japan

^b Graduate School of Engineering Science, Osaka University, 1-3 Machikaneyama-cho, Toyonaka, Osaka 560-8531, Japan

ARTICLE INFO

Article history:

Received 11 July 2014

Accepted 29 August 2014

Available online 16 September 2014

Keywords:

ECM (extracellular matrix)

Micropatterning

Fibronectin

Cell culture

Surface treatment

Polydimethylsiloxane

ABSTRACT

Cell-sheet-engineering based regenerative medicine is successfully applied to clinical studies, though cell sheets contain uniformly distributed cells. For the further application to complex tissues/organs, cell sheets with a multi-cellular pattern were highly demanded. Micro-contact printing is a quite useful technique for patterning proteins contained in extracellular matrix (ECM). Because ECM is a kind of cellular adherent molecules, ECM-patterned cell culture surface is capable of aligning cells on the pattern of ECM. However, a manual printing is difficult, because a stamp made from polydimethylsiloxane (PDMS) is easily deformed, and a printed pattern is also crushed. This study focused on the deformability of PDMS stamp and discussed an appropriate stamping force in micro-contact printing. Considering in availability in a medical or biological laboratory, a method for assessing the stamp deformability was developed by using stiffness measurement with a general microscope. An automated stamping system composed of a load cell and an automated actuator was prepared and allowed to improve the quality of stamped pattern by controlling an appropriate stamping force of 0.1 N. Using the system and the control of appropriate stamping force, the pattern of 8-mm-diameter 80- μ m-stripe fibronectin was fabricated on the surface of temperature-responsive cell culture dish. After cell-seeding and cell culture, a co-culture system with the micro-pattern of both fibroblasts and endothelial cells was completed. Furthermore, by reducing temperature to 20 °C, the co-cultured cell sheet with the micro-pattern was successfully harvested. As a result, the method would not only provide a high-quality ECM pattern but also a breakthrough technique to fabricate multi-cellular-patterned cell sheets for the next generation of regenerative medicine and tissue engineering.

© 2014 Elsevier Ltd. All rights reserved.

1. Introduction

For a decade, cell sheet transplantation is becoming one of key methods in regenerative medicine [1]. A cell sheet is a thin membrane composed of cultured cells and can be harvested from a temperature-responsive cell-culture dish by simply lowering temperature [2]. Since a cell sheet format is suitable for transplanting plenty of cells onto the surface of tissues/organs like a patch, cell sheets are widely used for repairing the damaged tissues/organs such as the skin [3], cornea [4], myocardium [5], esophagus [6], lung [7] periodontal tissue [8], cartilage [9], and middle ear mucosa [10]. These cell sheets include only a single type of cells, and for example,

epithelial cells are used for repairing the skin, cornea, and esophagus, and muscle cells are used for the myocardium. On the other hand, although a cell-sheet imitating complex tissue such as liver [11] etc. have been attempted to be fabricated in several laboratories [12–15], they have been never used for actual clinic. Upon the demand of repairing the damaged complex tissues with cell sheets, a patterned multi-type-cell sheet is an essential material with a potential for transplants.

One of useful techniques for fabricating complex cell sheets is a protein patterning by micro-contact printing [16] and consequent cell spontaneous organization by the adhesion interaction between cells and proteins in extracellular matrix (ECM) [17]. In micro-contact printing, a protein on a stamp with a target pattern made from polydimethylsiloxane (PDMS) is transferred to the surface of cell culture dish. Generally, micro-contact printing is still manually operated [18]. However, this technique requires highly skillful

* Corresponding author.

E-mail addresses: tokano@twmu.ac.jp, tokano@abmes.twmu.ac.jp (T. Okano).

technicians who can adjust the stamping force adequately, because PDMS stamp is easily deformed by the stamping force [19]. When the deformation of stamp is too large to exceed the height of stamp pattern, of cause, the bottom of stamp attaches on the dish surface, resulting in an unsuccessful printing with over-size patterns. Therefore, ECM patterning by an automated system is highly demanded. When the automated system is used, an index for determining an appropriate stamping force should be required, and considered the relationship between stamping force and the deformation of PDMS stamp, namely the stiffness of PDMS stamp.

The effect of automated-device use is expected to improve the accuracies of stamping-force measurement and positioning PDMS stamp to an object surface with a level far higher than that of manual operation. Therefore, for improving the quality of printed ECM pattern, the combination of load cell, a kind of force sensor, and an automated stage with a positioning accuracy of micrometer order has been proposed to be a useful system in the authors' previous study [20]. The previous study also proposes methods for calibrating the stiffness of PDMS stamp and estimating an appropriate stamping force, and performs the preliminary experiment of micro-contact printing in a stamping force measurement. However, the fabrication of patterned co-cultured cell sheet never succeeds because of inadequate experimental conditions. Furthermore, there is no discussion about the applicable range of the calibration

method of stamp stiffness. Therefore, this study improved (1) an automated system for micro-contact printing and (2) the calibration method with considering in the stiffness of PDMS stamp for the automation of micro-contact printing for increasing its applicability. First, a stiffness measurement method capable to evaluate the stiffness of stamp without any contact was introduced with the higher precision of measurement than that in the previous study. Then, the automated system was basically improved with (1) a fixation device keeping both PDMS stamp and cell culture dish in parallel and (2) the replacement of force sensor into a precise load cell. An equation for the index of stamping force was derived with the stiffness of stamp, and its efficacy was verified by using the automated system controlling the stamping force with various levels with a minimum resolution of 0.1 N. Finally, this study showed the fabrication of co-culture system that had a pattern with both endothelial cells and fibroblasts based on the stamping-force-controlled micro-contact printing of ECM (Fig. 1).

2. Materials and methods

2.1. Fabrication of PDMS stamp

PDMS stamps were fabricated by a modified method as the previous study [19]. Silicon wafers (p-type, approxi. 75 mm in diameter, 380 μm in thickness) (SEMITEC, Chiba, Japan) were treated with vacuum oxygen plasma for 3 min at an intensity of radio frequency of 400 W and oxygen pressure of 13 kPa in a chamber by using a

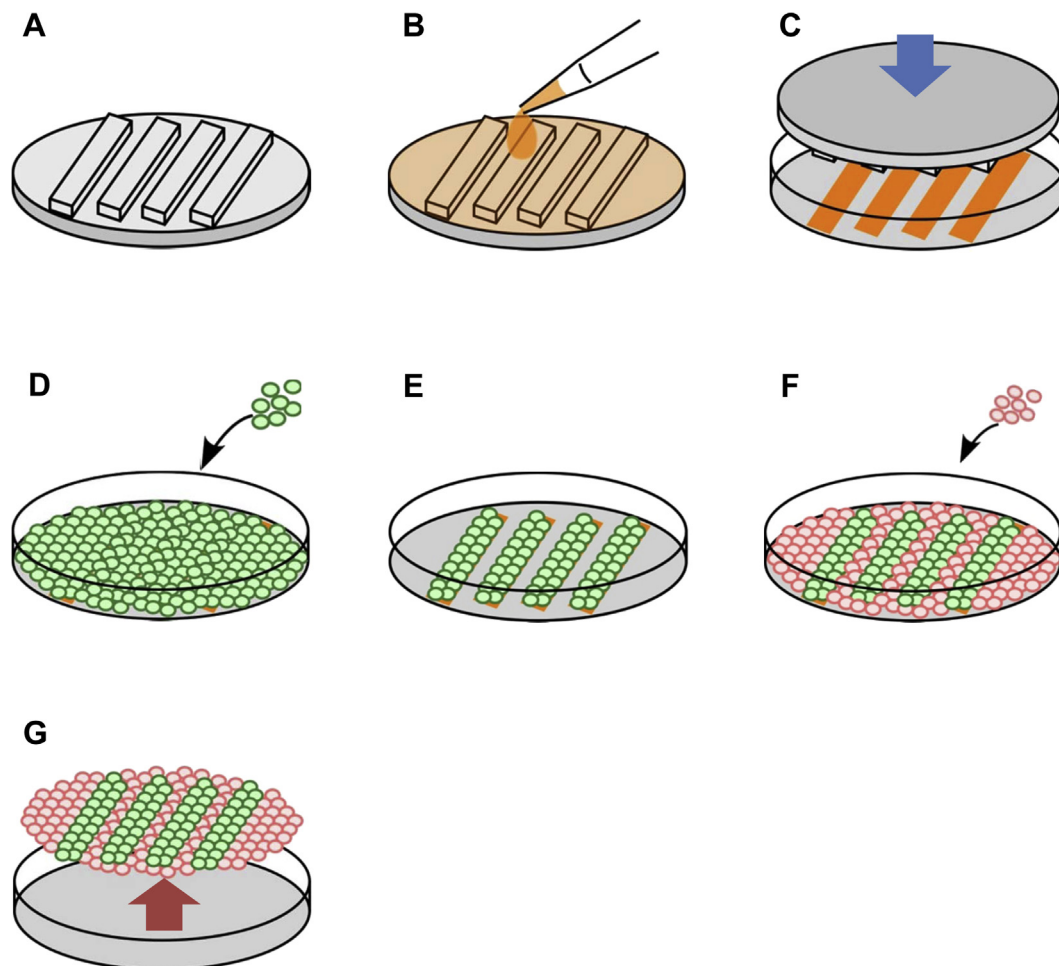


Fig. 1. Procedure for the fabrication of microstructured cell sheet by microcontact printing with stamping-force control. (A) Fabrication and inspection of polydimethylsiloxane (PDMS) stamp. (B) Application of extracellular matrix onto the surface of PDMS stamp. (C) Microcontact printing with appropriate stamping force. (D) Seeding the 1st cells. (E) Brief incubation and medium change. (F) Seeding 2nd cells. (G) After brief incubation, medium change, and cell culture, the harvest of cell sheet by reducing the temperature of temperature-responsive cell culture dish.

plasma cleaner (PC-1100) (SAMCO, Kyoto, Japan). The negative photoresist for visible light (405 nm) (SU-8 3050 G1) (Nippon Kayaku, Tokyo, Japan) was spin-coated onto the treated silicon wafers by using a spin coater (ACT-300D) (ACTIVE, Saitama, Japan) at 7000 rpm for 30 s. After being pre-baked for 1 h at 100 °C in a high-temperature chamber (ST-110) (ESPEC, Osaka, Japan), the photoresist on the silicon wafers was exposed with patterned visible light for 8 s by using a maskless exposure system previously reported [21]. An 80- μm -width and 200- μm -pitch stripe pattern was used for the exposure. The post-baking of photoresist was performed for 30 min at 80 °C and next for 30 min at 110 °C. After being cooled to room temperature, the photoresist was developed with 2-methoxy-1-methylethyl acetate (130–10,505) (Wako Pure Chemical, Osaka, Japan) over 1 h at room temperature. The developed surfaces were rinsed with ethanol (057–00451) (Wako) and dried with nitrogen gas blow. After being treated with vacuum oxygen plasma under the same condition for silicon wafers at the first, the surface were treated with 10 μL of trichloro(1H,1H,2H,2H-tridecafluoro-*n*-octyl)silane (T2577) (Tokyo Chemical Industry, Tokyo, Japan) for 30 min in a vacuum desiccator (1-5801-11) (AS ONE, Osaka, Japan) at 10 kPa. The treated surfaces were rinsed with ethanol and dried with nitrogen gas blow. After being degassed under vacuum drawing, a mixture of polydimethylsiloxane (PDMS) prepolymer and catalyst (Silpot 184) (Dow Corning Toray, Tokyo, Japan) was poured onto the treated surfaces, as a master mold, in a cell-culture dish (353,003) (Becton Dickinson, Franklin Lakes, NJ). The poured mixture of PDMS was cured for 1 h at 70 °C on a hot plate (NHP-M30N) (NISSIN, Tokyo, Japan). The cured PDMS was cut, peeled from the master mold, and trimmed out patterned area to provide an 8-mm-diameter stamp surface. After being rinsed with ethanol and dried with nitrogen gas blow, the back side of trimmed PDMS stamps and borosilicate cover glasses (25 mm in diameter, thickness No. 3) (Matsunami Glass, Osaka, Japan) were treated with vacuum oxygen plasma for 1 min at an intensity of radio frequency of 100 W and an oxygen pressure of 10 kPa in a chamber by using the plasma cleaner. Both treated surfaces of PDMS stamps and cover glasses were immediately bonded, and the bounded stamps and cover glasses were baked for 1 h at 70 °C on a hot plate (NEO HOTPLATE Hi-1000) (AS ONE). The surface shape of fabricated PDMS stamp was measured with a laser displacement sensor (CD5-L25) (OPTEX FA, Kyoto, Japan) (Fig. 1A).

2.2. Stiffness assessment of PDMS stamp

For obtaining the stiffness of PDMS stamp (item No. 3 in Fig. 2A), a stiffness measurement setup based on air-jet pressure application approach [22,23], which

consisted of main two parts; (1) an inverted microscope (ECLIPSE TE2000-U) (Nikon, Tokyo, Japan) for observing the deformation of stamp surface and (2) a force application device with a home-made transparent air-nozzle (item No. 2 in Fig. 2A), and a pressure regulator (IR2000) (SMC, Tokyo, Japan), was prepared. The inner diameter, outer diameter, and height of air-nozzle were 0.5, 2, and 10 mm, respectively (Fig. 2B). The air-nozzle was fabricated with biocompatible transparent resin (MED610) (Stratasys, Edina, MN) with a 3D printer (Objet Eden350V) (Stratasys). The air-nozzle was fixed under the condenser lens of microscope (item No. 1 in Fig. 2A) where the light axis of microscope coincided with the axis of nozzle hole. Compressed air was supplied from an air compressor (DPP-ATAD) (Kogaeni, Tokyo, Japan) to the air-nozzle and pass through a sterilization filter (VACU-GUARD, 6722-5000) (GE Healthcare UK, Buckinghamshire, UK), and then, air-jet was blown out from the air-nozzle. The distance between the nozzle and an object was adjusted to 2 mm by moving the condenser lens with the visual confirmation of focal plane via microscopic image. The relationship between the inlet and outlet of air-nozzle pressures was calibrated with a digital manometer (1-6121-01) (AS ONE) as previously described [20]. The applied pressure to PDMS stamp was assumed to be the same as the outlet pressure, which was estimated from the inlet pressure. In stiffness assessment, the various levels of air pressure generated by the air-jet were applied from the air-nozzle to the surface of PDMS stamp for over 1 min for making the PDMS stamp deformed. The surface of PDMS stamp was focused by the microscope at a specific pressure, and the focal position was measured at a resolution of 1 μm on the dial of microscope. The relative displacements of focal positions between with and without pressure application were calculated. The slope between the applied air pressure and the relative displacement was determined as the stiffness of PDMS stamp.

2.3. Micro-contact printing system

A micro-contact printing system was prepared for improving the quality of ECM printing. The system was composed of both a linear actuator (SGSP20-85(Z)), (SIGMAKOKI, Tokyo, Japan) (item No. 1 in Fig. 3A) and a force sensor (LUC-B-50N-ID-P) (KYOWA ELECTRONIC INSTRUMENTS, Tokyo, Japan) (item No. 2 in Fig. 3A). In the linear actuator, the position accuracy and the position resolution were 5 μm and 1 μm , respectively. The resolution of force sensor was 1 mN. The linear actuator and the force sensor were controlled by home-brewed software running on a desktop computer (HP Compaq dc5700 SFF) (Hewlett–Packard, Palo Alto, CA). The control

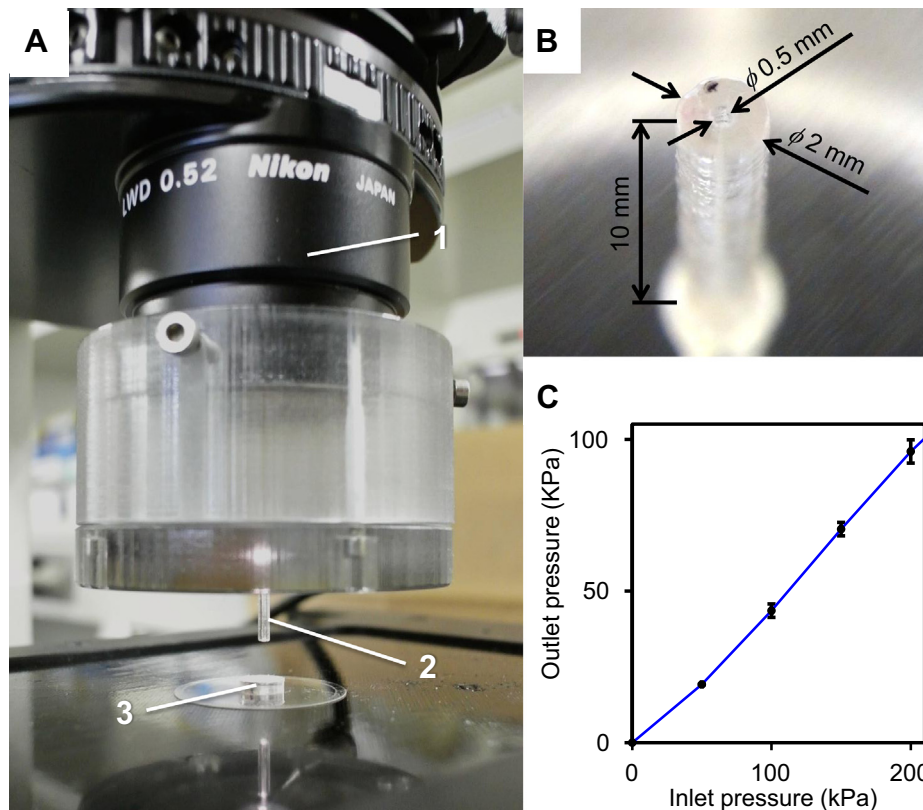


Fig. 2. Stiffness measurement setup. Photo (A) shows the composition of setup. (1) The condenser lens of an inverted phase-contrast microscope. (2) Transparent air-nozzle. (3) A measurement object. Photo (B) shows the magnified image of the transparent air-nozzle. Graph (C) shows the relationship between pressure applied by air-jet under the air-nozzle and supplied air pressure through the regulator. Data points and error bars are the value of average and standard deviations ($N = 3$), respectively.

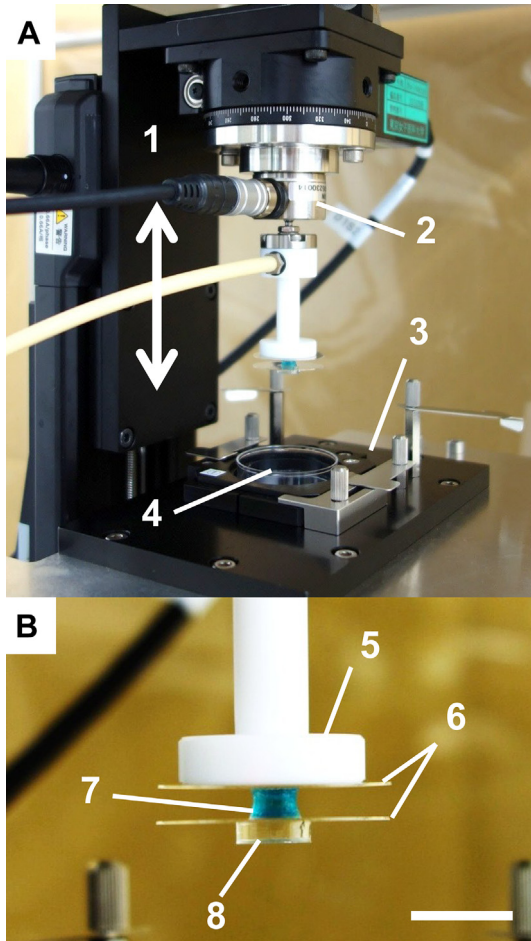


Fig. 3. Microcontact printing system. Photo (A) shows the overview of system; (1) a linear slider to the z-axis direction, (2) a load cell for measuring stamping force, (3) a holder for cell culture dish, and (4) a cell culture dish. Photo (B) shows the close-up view of system; (5) an end-effector for holding a polydimethylsiloxane (PDMS) stamp, (6) borosilicate cover glasses, (7) polyurethane gel, and (8) PDMS stamp. White bar indicates 1 cm.

cycle was 1 ms. A home-made vacuum suction probe was used for holding PDMS stamp at the tip of force sensor.

2.4. ECM application onto the stamp

ECM was applied onto the stamp surface by a modified method as the previous study [19], ECM was applied onto the stamp surface by a modified method as the previous study [19]. Dusts on PDMS stamps bonding with cover glass were carefully and gently removed with mending tape (MP-18) (Sumitomo 3M, Tokyo, Japan). The cleaned PDMS stamps were rinsed with ethanol and dried with nitrogen gas blow. After being treated with vacuum oxygen plasma for 3 min at an intensity of radio frequency of 400 W and an oxygen pressure of 13 kPa in a chamber of plasma cleaner, the surface were treated with the vapor of 10 μ L of trichloro(1H,1H,2H,2H-tridecafluoro-n-octyl)silane for 30 min in the vacuum desiccator under 10 kPa. The treated PDMS stamps were rinsed with ethanol and dried with nitrogen gas blow. Fibronectin derived from bovine plasma (F1141) (Sigma–Aldrich, St. Louis, MO) was diluted (100 μ g/mL) in Dulbecco's phosphate buffer saline (PBS) (D1408) (Sigma–Aldrich). The diluted fibronectin solution was applied and fully covered on the surface of PDMS stamp head perpendicularly. The solution-applied PDMS stamps were incubated in a petri dish (150,255) (Thermo Scientific, Roskilde, Denmark) to prevent the solution drying for 1 h at room temperature. The incubated PDMS stamps were immersed in sterilized and deionized water for 5 s. After water remaining on the PDMS stamps was blown by nitrogen gas, the PDMS stamps were used for printing (Fig. 1B).

2.5. Micro-contact printing with the system

A target temperature-responsive cell culture dish (UpCell[®]) (CellSeed, Tokyo, Japan) (item No. 4 in Fig. 3A) was fixed with a metal holder (item No. 3 in Fig. 3A) for

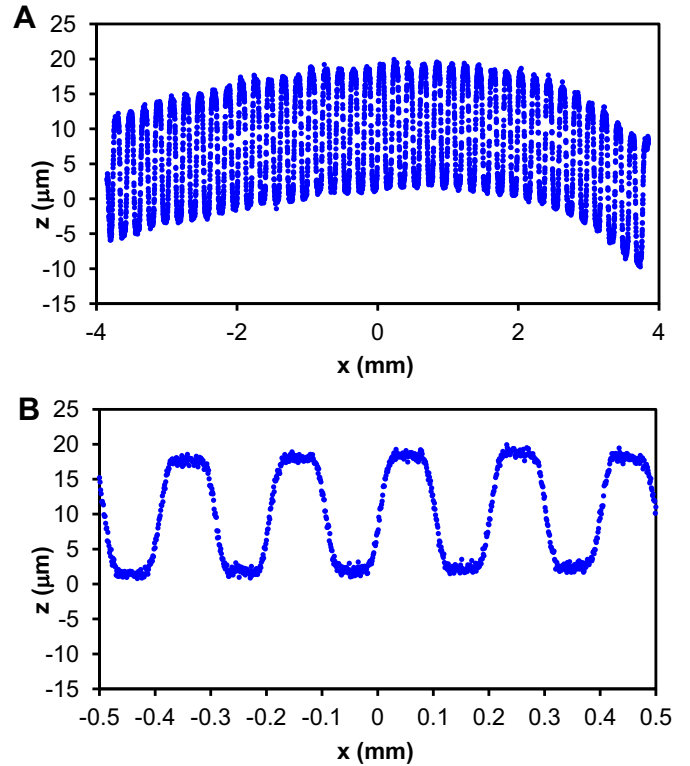


Fig. 4. The surface profiles of polydimethylsiloxane (PDMS) stamp. Graph (A) shows the cross-sectional surface profile of PDMS stamp measured by a scanning laser displacement sensor with a pitch of 1 μ m to x-axis direction. Graph (B) shows the magnified graph of surface profile around the center of PDMS.

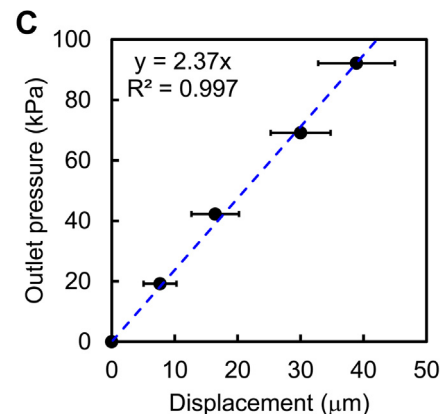
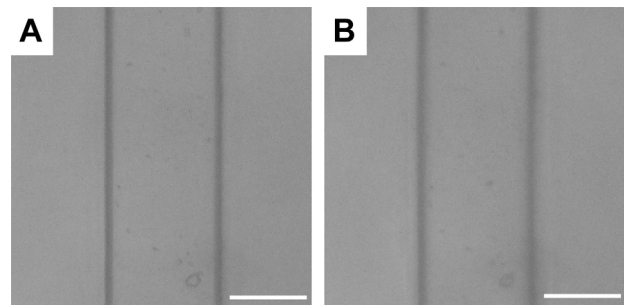


Fig. 5. Stiffness assessment of polydimethylsiloxane (PDMS) stamp. Microphotograph (A) and (B) show the surfaces of PDMS stamp at 0- and 92-kPa air pressure application, respectively. White bars indicate 200 μ m. (C) The relationship between pressure under the outlet of air-nozzle and the displacement of PDMS stamp. Data points and error bars are the value of average and standard deviations ($N = 6$), respectively. Dashed line indicates an approximation straight line with an intercept of the origin for the data points.

preventing a rattle of dish. A fibronectin-applied PDMS stamp was held by the tip of vacuum suction holder (item No. 5 in Fig. 3B) with a polyurethane elastomer column (outer diameter: 8 mm, height: 3 mm) (2184) (ACTY, Nagoya, Japan) (item No. 7 in Fig. 3B). The elastomer column was inserted between two borosilicate cover glasses (25 mm in diameter, thickness No. 3) (Matsunami) (item No. 6 in Fig. 3B). The surface of PDMS stamp (item No. 8 in Fig. 3B) was forced to be in contact to the target dish by moving down the linear slider. Contact force between the stamp and the dish was from 0.1 to 2.0 N. After a 1 min contact, PDMS stamp was detached by moving up the linear slider (Fig. 1C). The surface of dish after the contact was monitored with a fluorescent microscope (TE-2000U) (Nikon, Tokyo, Japan).

2.6. Fabrication of patterned cell sheet

Bovine aortic endothelial cells (BAEC) (JCRB0099 HH) (JCRB Cell Bank, Osaka Japan) and normal human epidermal fibroblasts (NHDF) (CC-2511) (TAKARA BIO, Shiga, Japan) were suspended in Dulbecco's Modified Eagle Medium (DMEM, D6429) (Sigma–Aldrich, St. Louis, MO) with 1v/v% antibiotics (penicillin-streptomycin, Gibco 15140-122) (Life Technologies, Carlsbad, CA) and Fibroblast Growth Medium 2 Kit (C-23120) (TAKARA BIO, Shiga, Japan), respectively. NHDF were stained with green-fluorescent dye [CellTracker Green CMFDA (5-Chloromethylfluorescein Diacetate)] (C7025) (Life Technologies) in advance of seeding cells. After fibronectin was printed on the dish (Fig. 1C), NHDF were firstly seeded into the dish (Fig. 1D). The seeded cells were cultured for 3 h in a humidified condition with 5% CO₂. After medium containing non-adherent cells was removed from the dish (Fig. 1E), BAEC were secondarily seeded into the dish (Fig. 1F). The initial densities of seeding NHDF and BAEC were 1.2×10^5 cells/cm². After a 1 h incubation, medium containing non-adherent cells was removed from the dish, and then, DMEM containing the antibiotics and 10% fetal bovine serum (FBS) (Lot No.

83300124) (Moregate BioTech, Queensland, Australia) was poured into the dish. After a 1-day cultivation, the dish surface was monitored with the fluorescent microscope, and a cell sheet containing BAEC and NHDF was recovered by reducing temperature to 20 °C (Fig. 1G). The recovered cell sheet was monitored with the fluorescent microscope.

3. Results and discussion

3.1. Surface profile of PDMS stamp

By using the laser displacement sensor, the surface profile of PDMS stamp was measured (Fig. 4A). The measured data was able to show both global and local profiles. In the trend of global surface profile, the surface was found to have a convex shape where the center of PDMS stamp was the bottom of convex part. The depth between the bottom of convex part and the upper part of PDMS stamp was found to be $12 \pm 3 \mu\text{m}$ (mean \pm SD) ($N = 3$). In the trend of local surface profile, the surface was fully covered with small convex and concave shapes caused by the stripe pattern on PDMS stamp. The local depth between the top and bottom of stripe pattern was measured to be $19 \pm 1 \mu\text{m}$ (mean \pm SD) ($N = 3$) (Fig. 4B). These results suggested that by not only contacting but also pushing the stamp to object surface with exceeded additional force, an excessive stamping force allowed the bottom part of stamp to hit

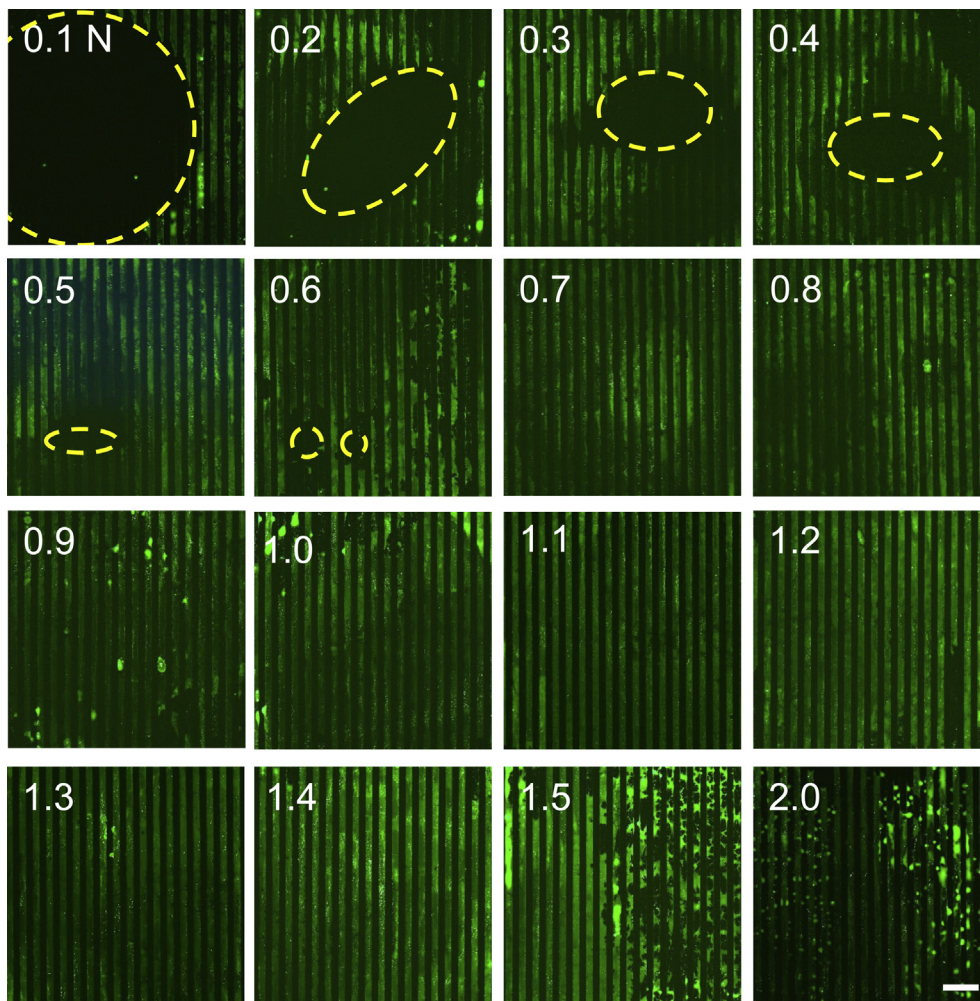


Fig. 6. Low-magnified fluorescent microphotographs of microcontact printed surface with the various levels of stamping force. The value in each image shows the level of stamping force. Yellow dashed line ellipses indicate the absence of printed pattern on the surface. Scale bar indicates 500 μm , and the scale of each image is the same. (For interpretation of the references to color in this figure legend, the reader is referred to the web version of this article.)

the object surface. Furthermore, the permissible value of stamp displacement was no more than 3 μm .

3.2. Stiffness assessment of PDMS stamp

The relationship between outlet and inlet pressures was found to be linear passing the origin (Fig. 2C). The outlet pressure was two times smaller than the inlet pressure adjusted by the pressure regulator. The reproducibility of pressure application by air-jet was high with a coefficient of variance $\pm 5\%$. Especially, the reproducibility at the range of lower pressure was higher than that at higher pressure, because the standard deviation at 50 kPa, the smallest inlet pressure, was 0. Therefore, in this setup, the pressure application by air-jet was speculated to be suitable for stiffness assessment of PDMS stamp, and the pressure applied to the surface of PDMS stamp was supposed to be the calibrated outlet pressure.

Upon the consideration of the measurement error of displacement generated by focusing error, generally, the possible range where an object focused image in this study was defined as the depth of focus d as follow:

$$d = \frac{250,000\omega}{\text{NA} \cdot M} + \frac{\lambda}{2\text{NA}^2} \quad (1)$$

where ω , NA, M , and λ are the resolution of human eye ($= 0.0014$), the numerical aperture of objective lens, the total magnification of microscope [$= 40$ (objective lens) $\times 10$ (eyepiece) $= 400$], and the wavelength of light ($= 0.55 \mu\text{m}$), respectively (Berek's formula [24]). In this study, 40 \times objective lens (S Plan Fluor ELWD ADM 40 \times), (Nikon, Tokyo, Japan) was attached to the microscope and showed NA = 0.6. Under this condition, $d = 2.2 \mu\text{m}$. Therefore, in this study, the displacement of object was able to be measured easily without a focusing error of over 5 μm . Naturally, errors caused by focusing were expected to depend on the skill of measurer. The error would be suppressed by using an automated focusing system [25,26].

Based on the error evaluation on both pressure application by air-jet and displacement measurement with the microscope, this setup was useful for assessing the stiffness of soft materials similar to PDMS simply, because one of main components, an inverted microscope, were found easily in medical laboratory investigating tissue engineering and regenerative medicine, and the 3D data of transplant nozzle was in public domain [27].

Without air-jet application, well-aligned stripe patterns on the surface of PDMS stamp were observed in focus (Fig. 5A). On the other hand, during air-jet application, the stamp surface was deformed by the pressure of air-jet. And then, the edge of stripe was out of focus (Fig. 5B). After the edge was refocused during air-jet

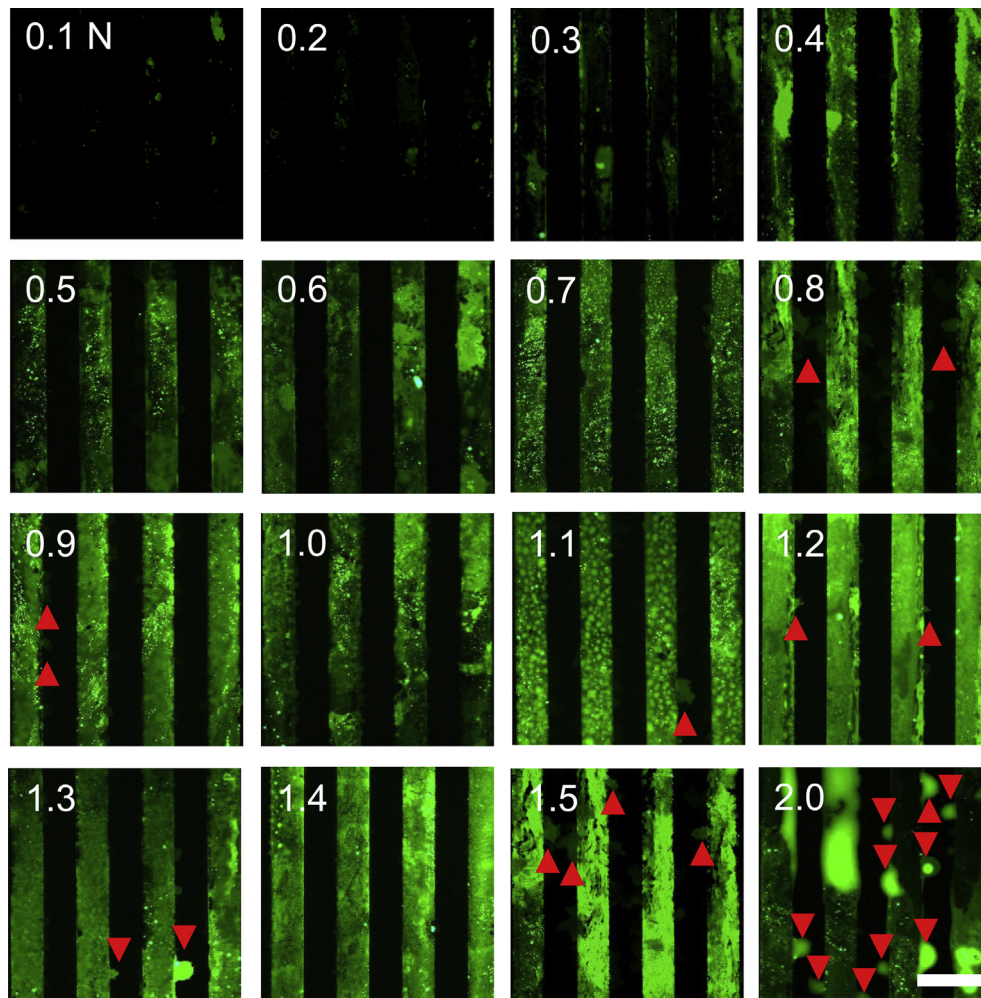


Fig. 7. High-magnified fluorescent microphotographs of microcontact printed surface with the various levels of stamping force. The value in each image shows the level of stamping force. Red arrowheads indicate the excessive area of printed pattern on the surface. Scale bar indicates 200 μm , and the scale of each image is the same. (For interpretation of the references to color in this figure legend, the reader is referred to the web version of this article.)

application, the relative displacement of PDMS stamp surface to the original surface before air-jet application was determined. In the stiffness assessment, the deformation of center part of microphotograph was used. The deformation was found to increase linearly as increasing the pressure of air-jet (Fig. 5C). This linear property was speculated to be caused by the infinitesimal deformation, because the maximum displacement of PDMS stamp in stiffness measurement was less than 50 μm , which was smaller than 20% thickness of PDMS stamp, and the complexity of deformation, such as the contribution of shear stress, was able to be negligible. The stiffness calculated from the slope of measured data was $2.4 \pm 0.4 \text{ kPa}/\mu\text{m}$ (mean \pm SD). Although this stiffness index was different from Young's modulus [28] and inapplicable to general purposes, one of the most general indexes of physical value, the value could provide the expected value of deformation during contact printing with a specified stamping force. This value indicated an 8-mm-diameter plane PDMS stamp with the same value of stiffness was expected to be deformed by 100-gram-load with a maximum displacement of 10 μm .

As the result of stiffness assessment, an appropriate stamping force was required, because the contact between the convex parts of stamp pattern and the target surface became neither too much

nor too little. Therefore, as one of the best methods for determining the appropriate stamping force, the squeezing distance between the edge of PDMS stamp and the bottom of globally concave part was only deformed. Under this assumption, the appropriate stamping force f was provided as follows:

$$f = krAh \quad (2)$$

where k , r , A , and h were the stiffness of PDMS stamp (in other words, the slope between the applied air pressure and the relative displacement of PDMS stamp), the ratio of the area of target pattern to the total area of stamp, the total area of stamp, and the appropriate deformation based on the error to the height direction on the stamp, respectively. The stiffness parameter of stamp k was able to be obtained from the result from the stiffness measurement. The geometric parameters of stamp r and A were design values. Another geometric parameter h was empirically given 4–5 μm from an observed value in the experimental conditions. The distance was able to be determined by a calculation with known values k , measured values h , and designed values r , and A , while both shape and stiffness assessments were performed.

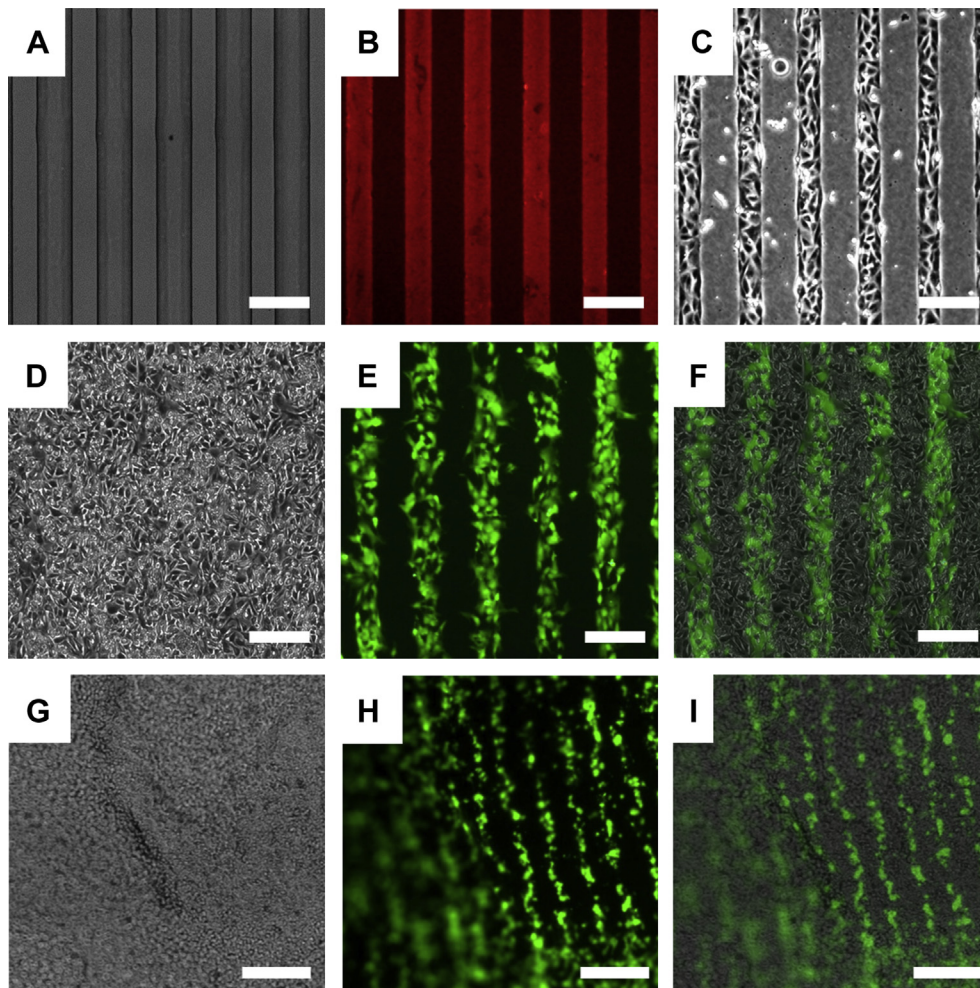


Fig. 8. Fabrication of microstructured cell sheet based on extracellular-matrix patterning by microcontact printing system. Microphotographs (A), (B), and (C) show the phase-contrast image of polydimethylsiloxane stamp surface with micro-pattern, the fluorescent image of rhodamine-fibronectin-printed surface, and the phase-contrast image of surface after seeding normal human dermal fibroblast (NHDF), respectively. Microphotographs (D), (E), and (F) show the phase contrast, fluorescent, and merged images of surfaces after seeding NHDF (green) and bovine artery endothelial cells, respectively, and white bars indicate 200 mm in (A)–(F) and 500 mm in (G)–(I). (For interpretation of the references to color in this figure legend, the reader is referred to the web version of this article.)

3.3. Printing quality in the various level of stamping force

With a small stamping force of less than 0.6 N, the printed pattern was observed with large defect areas (Fig. 6). Especially, the defect areas were located at a region near to the center, because the convex shape of PDMS stamp directly affected the contact of surfaces between PDMS stamp and target dish (Fig. 4A). On the other hand, by a stamping force of over 0.7 N, no defect was observed (Fig. 6). However, in magnified microphotographs (Fig. 7), an excessive stamping force of over 0.8 N was found to provide extruded parts from printed pattern. These results were speculated to be caused by an interaction among the curved surface of stamp, the height of formed patterns, and PDMS stiffness. As a result, the quality of printed patterns strongly depended on the level of stamping force, because only printed pattern at 0.7 N had the best quality in the experimental results. The value of appropriate stamping force for PDMS stamp used in this experiment was calculated, from the equation (2), to be $f = 0.72$ N in the case of $k = 2.4$ kPa/ μm , $r = 0.4 = 80/200$ (= width/pitch), $A = 5.0 \times 10^{-5}$ m² ($=\pi/4 \times \text{diameter}^2$), $h = 15$ μm (= mean + max. range). And, the calculated value was the same as the value of stamping force giving the best quality of printed pattern in the experimental data. The variation of stiffness index of PDMS stamp was within 17%. The range of stamping force corresponding to the standard deviation between 0.6 and 0.8 N never produced destructive patterns including 10%-under/over printed area, similar to the patterns in 0.1 or 2.0 N (Figs. 6 and 7). Furthermore, in the preliminary experiment described in the reference [20], the estimated value of appropriate stamping force even in rough estimation also provides better-printed patterns among those in the cases of the other stamping forces, though the experimental setup is simpler than that of the current study. Therefore, the stiffness index derived from the stiffness measurement method was robust for determining the appropriate stamping force. These results indicated that (1) micro-contact printing had essentially a difficulty, which was affected by the elasticity of PDMS, and (2) the difficulty was able to be overcome easily by controlling an appropriate stamping force with a resolution of 0.1 N, which was based on the simple method for the stiffness assessment with air-jet and a microscope, even without special instruments.

3.4. Micro-patterned cell sheet

With an appropriate stamping force, rhodamine-fibronectin was successfully transferred from a stripe-pattern-formed PDMS stamp (Fig. 8A) onto the surface of temperature-responsive cell culture dish (Fig. 8B). After NHDF were seeded and unattached cells were removed, the cells were observed to be aligned in the same manner as the stripe pattern of fibronectin (Fig. 8C). Furthermore, after the second cells were seeded, the surface of dish was fully covered with both cells (Fig. 8D). On the same dish, the stripe pattern cover of the first seeded cells was still remained in the fluorescent microphotograph (Fig. 8E and F). After lowering temperature, the cells were successfully detached from the dish surface as a continuous cell sheet, which was observed to float in culture medium (Fig. 8G). In the fluorescent microphotograph, the stripe pattern composed of green-fluorescent-dye-stained NHDF and unstained BAEC was found to be still preserved in the harvested cell sheet (Fig. 8G and H). Because the cell sheet was floating in the medium and slightly curved, some areas were out of focus in the microphotographs (Fig. 8G–I). As a result, the fabrication of cell sheets with patterns consisting of two different types of cells was succeeded. Especially, endothelial cell and fibroblast were quite important cells in non-parenchymal cells for maintaining the inherent functions of complex organ and tissues such as liver [29–31]. Therefore, the

patterned cell sheets would be useful as a supportive tissue in the case of layered cell sheet composed of parenchymal cells.

4. Conclusion

This study proposed a simple calibration method for measuring PDMS stamp stiffness for providing an appropriate stamping force in micro-contact printing. Force control by the developed system was able to fabricate a high-quality printed pattern of fibronectin. A cell sheet composed of endothelial cells and fibroblasts was successfully fabricated with stable micro-contact-printing-based fibronectin patterning. This method would be useful for fabricating a micro-patterned cell sheet in both tissue engineering and regenerative medicine for the complex tissues and organs.

Acknowledgments

The study was supported by the Formation of Innovation Center for Fusion of Advanced Technologies in the Special Coordination Funds for Promoting Science and Technology “Cell Sheet Tissue Engineering Center (CSTEC)” from the Ministry of Education, Culture, Sports, Science and Technology (MEXT), Japan, Grant-in-Aid for Scientific Research on Innovative Areas “Hyper Bio Assembler for 3D Cellular Innovation” from the MEXT, the Global Center of Excellence Program, Multidisciplinary Education and Technology and Research Center for Regenerative Medicine (MERCREM) from the MEXT, and Grant-in-Aid for Japan Society for the Promotion of Science (JSPS) Fellows (23·7758) from JSPS. We are grateful to Dr. Norio Ueno for English editing. Teruo Okano is a founder and director of the board of CellSeed Inc., licensing technologies and patents from Tokyo Women’s Medical University. Teruo Okano and Masayuki Yamato are stake holders of CellSeed Inc. Tokyo Women’s Medical University is receiving research fund from CellSeed Inc.

References

- [1] Yang J, Yamato M, Shimizu T, Sekine H, Ohashi K, Kanzaki M, et al. Reconstruction of functional tissues with cell sheet engineering. *Biomaterials* 2007;28:5033–43.
- [2] Yamada N, Okano T, Sakai H, Karikusa F, Sawasaki Y, Sakurai Y. Thermoresponsive polymeric surfaces; control of attachment and detachment of cultured cells. *Die makromolekulare chemie. Rapid Commun* 1990;11:571–6.
- [3] Yamato M, Utsumi M, Kushida A, Konno C, Kikuchi A, Okano T. Thermoresponsive culture dishes allow the intact harvest of multilayered keratinocyte sheets without disperse by reducing temperature. *Tissue Eng* 2001;7:473–80.
- [4] Nishida K, Yamato M, Hayashida Y, Watanabe K, Yamamoto K, Adachi E, et al. Corneal reconstruction with tissue-engineered cell sheets composed of autologous oral mucosal epithelium. *N Engl J Med* 2004;351:1187–96.
- [5] Shimizu T, Yamato M, Kikuchi A, Okano T. Cell sheet engineering for myocardial tissue reconstruction. *Biomaterials* 2003;24:2309–16.
- [6] Ohki T, Yamato M, Ota M, Takagi R, Murakami D, Kondo M, et al. Prevention of esophageal stricture after endoscopic submucosal dissection using tissue-engineered cell sheets. *Gastroenterology* 2012;143:582–8.
- [7] Kanzaki M, Yamato M, Yang J, Sekine H, Kohno C, Takagi R, et al. Dynamic sealing of lung air leaks by the transplantation of tissue engineered cell sheets. *Biomaterials* 2007;28:4294–302.
- [8] Iwata T, Yamato M, Tsuchioka H, Takagi R, Mukobata S, Washio K, et al. Periodontal regeneration with multi-layered periodontal ligament-derived cell sheets in a canine model. *Biomaterials* 2009;30:2716–23.
- [9] Sato M, Yamato M, Hamahashi K, Okano T, Mochida J. Articular cartilage regeneration using cell sheet technology. *Anat Rec* 2013;297:36–43.
- [10] Yaguchi Y, Murakami D, Yamato M, Hama T, Yamamoto K, Kojima H, et al. Middle ear mucosal regeneration with three-dimensionally tissue-engineered autologous middle ear cell sheets in rabbit model. *J Tissue Eng Regen Med* 2013. <http://dx.doi.org/10.1002/term.1790>.
- [11] Michalopoulos GK, DeFrances MC. Liver regeneration. *Science* 1997;276:60–6.
- [12] Yamato M, Konno C, Utsumi M, Kikuchi A, Okano T. Thermally responsive polymer-grafted surfaces facilitate patterned cell seeding and co-culture. *Biomaterials* 2002;23:561–7.
- [13] Ohashi K, Yokoyama T, Yamato M, Kuge H, Kanehiro H, Tsutsumi M, et al. Engineering functional two- and three-dimensional liver systems in vivo using hepatic tissue sheets. *Nat Med* 2007;13:880–5.

- [14] Ota H, Kodama T, Miki N. Rapid formation of size-controlled three dimensional hetero-cell aggregates using micro-rotation flow for spheroid study. *Biomicrofluidics* 2011;5:34105–3410515.
- [15] Takebe T, Sekine K, Enomura M, Koike H, Kimura M, Ogaeri T, et al. Vascularized and functional human liver from an iPSC-derived organ bud transplant. *Nature* 2013;499:481–4.
- [16] Kane RS, Takayama S, Ostuni E, Ingber DE, Whitesides GM. Patterning proteins and cells using soft lithography. *Biomaterials* 1999;20:2363–76.
- [17] Elloumi Hannachi I, Itoga K, Kumashiro Y, Kobayashi J, Yamato M, Okano T. Fabrication of transferable micropatterned-co-cultured cell sheets with microcontact printing. *Biomaterials* 2009;30:5427–32.
- [18] Elloumi-Hannachi I, Maeda M, Yamato M, Okano T. Portable microcontact printing device for cell culture. *Biomaterials* 2010;31:8974–9.
- [19] Qin D, Xia Y, Whitesides GM. Soft lithography for micro- and nanoscale patterning. *Nat Protoc* 2010;5:491–502.
- [20] Tanaka N, Ota H, Fukumori K, Yamato M, Okano T. Stamp-stiffness calibrated micro contact printing. *IEEE Int Conf Robot Autom* 2013;2567–72.
- [21] Itoga K, Kobayashi J, Tsuda Y, Yarnato M, Okano T. Second-generation maskless photolithography device for surface micropatterning and microfluidic channel fabrication. *Anal Chem* 2008;80:1323–7.
- [22] Tanaka N, Higashimori M, Kaneko M, Imin K. Noncontact active sensing for viscoelastic parameters of tissue with coupling effect. *IEEE Trans Biomed Eng* 2011;58:509–20.
- [23] Tanaka N, Kondo M, Uchida R, Kaneko M, Sugiyama H, Yamato M, et al. Splitting culture medium by air-jet and rewetting for the assessment of the wettability of cultured epithelial cell surfaces. *Biomaterials* 2013;34:9082–8.
- [24] Brattgard SO. Microscopical determinations of the thickness of histological sections. *J R Microsc Soc* 1954;74:113–22.
- [25] Groen FC, Young IT, Ligthart G. A comparison of different focus functions for use in autofocus algorithms. *Cytometry* 1985;6:81–91.
- [26] Nguyen CN, Ohara K, Mae Y, Arai T. High-speed focusing and tracking of multisized microbiological objects. *J Robot Mechatronics* 2013;25:115–24.
- [27] Transparent air-nozzle, <http://www.thingiverse.com/thing:448099>.
- [28] Armani D, Liu C, Aluru N. Re-configurable fluid circuits by PDMS elastomer micromachining. *IEEE Proc Int Conf MEMS* 1999;222–7.
- [29] Bhatia SN, Balis UJ, Yarmush ML, Toner M. Effect of cell-cell interactions in preservation of cellular phenotype: cocultivation of hepatocytes and non-parenchymal cells. *FASEB J* 1999;13:1883–900.
- [30] Yamada M, Utoh R, Ohashi K, Tatsumi K, Yamato M, Okano T, et al. Controlled formation of heterotypic hepatic micro-organoids in anisotropic hydrogel microfibers for long-term preservation of liver-specific functions. *Biomaterials* 2012;33:8304–15.
- [31] Kobayashi A, Yamakoshi K, Yajima Y, Utoh R, Yamada M, Seki M. Preparation of stripe-patterned heterogeneous hydrogel sheets using microfluidic devices for high-density coculture of hepatocytes and fibroblasts. *J Biosci Bioeng* 2013;116:761–7.